DOI: 10.1002/ange.201001839

VIP Nanostructures

A Sinter-Resistant Catalytic System Based on Platinum Nanoparticles Supported on TiO_2 Nanofibers and Covered by Porous Silica**

*Yunqian Dai, Byungkwon Lim, Yong Yang, Claire M. Cobley, Weiyang Li, Eun Chul Cho, Benjamin Grayson, Paul T. Fanson, Charles T. Campbell, Yueming Sun, and Younan Xia**

Platinum is a key catalyst that is invaluable in many important industrial processes such as CO oxidation in catalytic converters, oxidation and reduction reactions in fuel cells, nitric acid production, and petroleum cracking.[1] Many of these applications utilize Pt nanoparticles supported on oxides or porous carbon.[2] However, in practical applications that involve high temperatures (typically higher than 300 °C), the Pt nanoparticles tend to lose their specific surface area and thus catalytic activity during operation because of sintering. Recent studies have shown that a porous oxide shell can act as a physical barrier to prevent sintering of unsupported metal nanoparticles and, at the same time, provide channels for chemical species to reach the surface of the nanoparticles, thus allowing the catalytic reaction to occur. This concept has been demonstrated in several systems, including Pt@SiO_2,[3] Pt@CoO,[4] Pt/CeO_2@SiO_2,[5] Pd@SiO_2,[6] Au@SiO_2,[7] Au@SnO_2[8] and Au@ZrO_2[9] core–shell nanostructures. Despite these results, a sinter-resistant system has not been realized in supported Pt nanoparticle catalysts.

Improved catalytic or photocatalytic properties are often achieved when metal nanoparticles are supported on oxides such as TiO_2 and CeO_2 that interact strongly with late transition metals.[2f,5] Herein, we demonstrate a thermally stable catalytic system consisting of Pt nanoparticles that are supported on a TiO_2 nanofiber and coated with a porous SiO_2 sheath. In this system, the porous SiO_2 coating offers an energy barrier to prevent the migration of individual Pt atoms or nanoparticles because of its weak interaction with late transition metals, including Pt. The porous-SiO_2/Pt/TiO_2 catalytic system was prepared in three steps (Figure 1): 1) deposition of Pt nanoparticles onto the surface of TiO_2 nanofibers; 2) coating of SiO_2 with cetyltrimethylammonium bromide (CTAB) as a pore-generating agent; and 3) calcination in air to generate a porous sheath of SiO_2. By using this approach, we were able to produce a platinum-based catalytic system that can resist sintering up to 750 °C in air, while retaining the catalytic activity of the Pt nanoparticles.

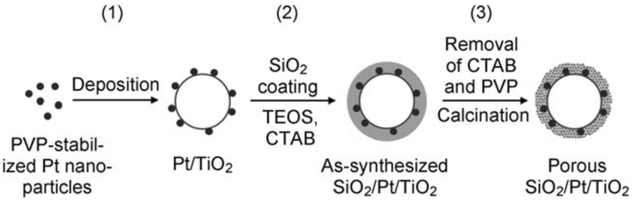

Figure 1. Preparation of the catalytic system based on Pt nanoparticles that are supported on TiO_2 nanofibers and then covered by porous sheaths of SiO_2: 1) deposition of PVP-stabilized Pt nanoparticles onto the surface of TiO_2 nanofibers; 2) formation of SiO_2 coating by the Stöber method; and 3) removal of CTAB and PVP by calcination in air to generate a porous sheath of SiO_2.

The TiO_2 nanofibers were prepared by electrospinning and subsequent calcination in air at 750 °C for 2 hours.[10] The as-prepared nanofibers had a rough surface and a polycrystalline structure that contained both anatase and rutile phases (69 % anatase and 31 % rutile; Figure S1 in the Supporting Information). Poly(vinyl pyrrolidone) (PVP) stabilized Pt nanoparticles were prepared by using the polyol method.[11] The as-synthesized Pt nanoparticles were uniform in size, with an average size of (3.1 ± 0.5) nm (Figure 2 a,b). These Pt nanoparticles were deposited onto the TiO_2 nanofibers by immersing the sample in a suspension of the Pt nanoparticles, which was prepared by a 10-fold dilution of the as-prepared Pt sample with ethanol. As shown in Figure 2 c, the Pt nanoparticles were well dispersed on the surface of each TiO_2 nanofiber, without significant aggregation. The Pt loading in the Pt/TiO_2 nanofibers was 1.3 wt %, as determined by inductively coupled plasma mass spectrometry (ICP-MS) measurements. Figure 2 d shows a high-resolution TEM

---

[*] Y. Dai, Dr. B. Lim, C. M. Cobley, W. Li, Dr. E. C. Cho, Prof. Y. Xia
Department of Biomedical Engineering
Washington University, St. Louis, MO 63130 (USA)
E-mail: xia@biomed.wustl.edu

Y. Dai, Prof. Y. Sun
School of Chemistry and Chemical Engineering
Southeast University, Nanjing, Jiangsu 211189 (P. R. China)

Dr. Y. Yang, Prof. C. T. Campbell
Department of Chemistry, University of Washington
Seattle, WA 98195 (USA)

Dr. B. Grayson, Dr. P. T. Fanson
Toyota Motor Engineering & Manufacturing North America, Inc.
Ann Arbor, MI 48105 (USA)

[**] This work was supported by the Toyota Motor Engineering & Manufacturing North America, Inc. Part of the research was performed at the Nano Research Facility (NRF), a member of the National Nanotechnology Infrastructure Network (NNIN) that is funded by the National Science Foundation under award no. ECS-0335765. As a visiting graduate student from Southeast University, Y.D. was also partially supported by the National Basic Research Program (973 program, 2007CB936300), the Innovation Program for Graduate Students in Jiangsu Province (CX08B-051Z), and the China Scholarship Council. We thank Prof. Jimmy Liu at the University of Missouri (St. Louis) for helping us with the sintering experiments under hydrogen gas.

Supporting information for this article is available on the WWW under http://dx.doi.org/10.1002/anie.201001839.

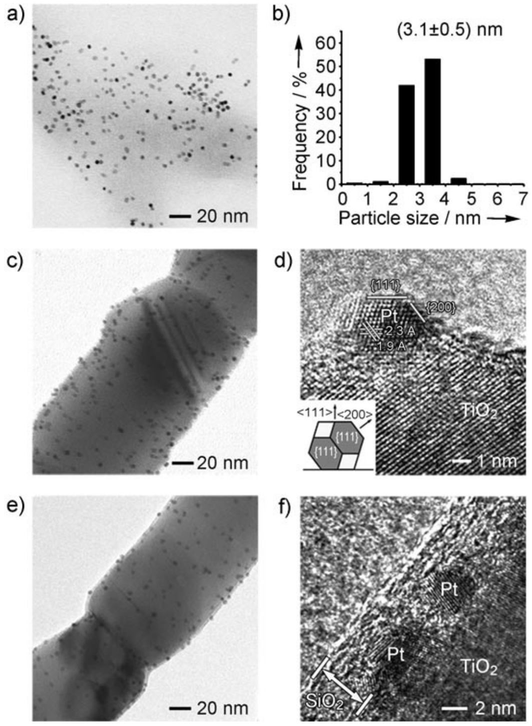

Figure 2. a) TEM image of PVP-stabilized Pt nanoparticles synthesized using the polyol method and b) the corresponding particle size distribution obtained by counting 150 particles in the TEM images. c) TEM and d) HRTEM images taken from the Pt/TiO_2 nanofiber sample prepared by immersing the calcined TiO_2 nanofibers in a suspension of the Pt nanoparticles. The inset in (d) shows a schematic model of a Pt truncated octahedron on the TiO_2 surface. e) TEM and f) HRTEM images taken from the sample that was obtained by coating the Pt/TiO_2 nanofibers shown in (c) with SiO_2 sheaths 4–6 nm thick.

(HRTEM) image of a single Pt nanoparticle on a TiO_2 nanofiber recorded along the [011] zone axis. The Pt nanoparticle exhibited a truncated octahedral shape with exposed {111} and {100} facets. The fringe spacing of 1.9 Å and 2.3 Å correspond to the {200} and {111} planes of face-centered cubic Pt, respectively.[1b] The Pt/TiO_2 nanofibers were then coated with SiO_2 sheaths by using a modified Stöber method,[12] in which CTAB was used as a pore-generating agent. The TEM analysis showed that a uniform SiO_2 coating with a thickness of 4–6 nm was formed on the surface of each Pt/TiO_2 nanofiber (Figure 2e). The HRTEM image in Figure 2f clearly shows that the thin SiO_2 sheath covered both the TiO_2 nanofiber and the Pt nanoparticles and that its thickness was uniform. We did not observe the formation of isolated SiO_2 particles in the product in both TEM and HRTEM analyses.

The as-prepared SiO_2/Pt/TiO_2 sample contains CTAB within the SiO_2 sheaths and the Pt nanoparticles are surrounded by PVP. These organic species can be removed from the SiO_2/Pt/TiO_2 nanofibers by calcination in air at 350 °C to generate porous SiO_2 sheaths.[2g,13] The TEM image and particle size analyses of the calcined porous-SiO_2/Pt/TiO_2 nanofibers revealed that the Pt nanoparticles did not form aggregates and retained small sizes with an average size of (3.5 ± 0.8) nm (Figure 3a). We also proved that the Pt surface in these materials was accessible to reactants by measuring the Pt surface area using selective chemisorption (CO titration of O adatoms; reference [14]). For several samples before (Figure 2c) and after (Figure 3a) silica coating, the average Pt dispersions were measured to be 42 % and 29 %, respectively. These dispersions are very close to the value of 39 %, which was estimated using the average diameter of 3.5 nm from TEM, assuming that the spherical particles have the same surface packing density as Pt(111), that is, 1.5×10^{15} Pt atoms per cm^2 (representative titration curves and surface areas are shown in Figure S2 in the Supporting Information).

Notably, the Pt nanoparticles did not exhibit a morphological change upon calcination at temperatures up to 750 °C (Figure 3b,c). However, in sharp contrast, the Pt nanoparticles were observed to aggregate in the absence of SiO_2 sheaths at all temperatures in the range 350–750 °C (Figure 3d–f). At 750 °C, the Pt nanoparticles aggregated extensively to form particles larger than 20 nm in size (Figure 3f). These results

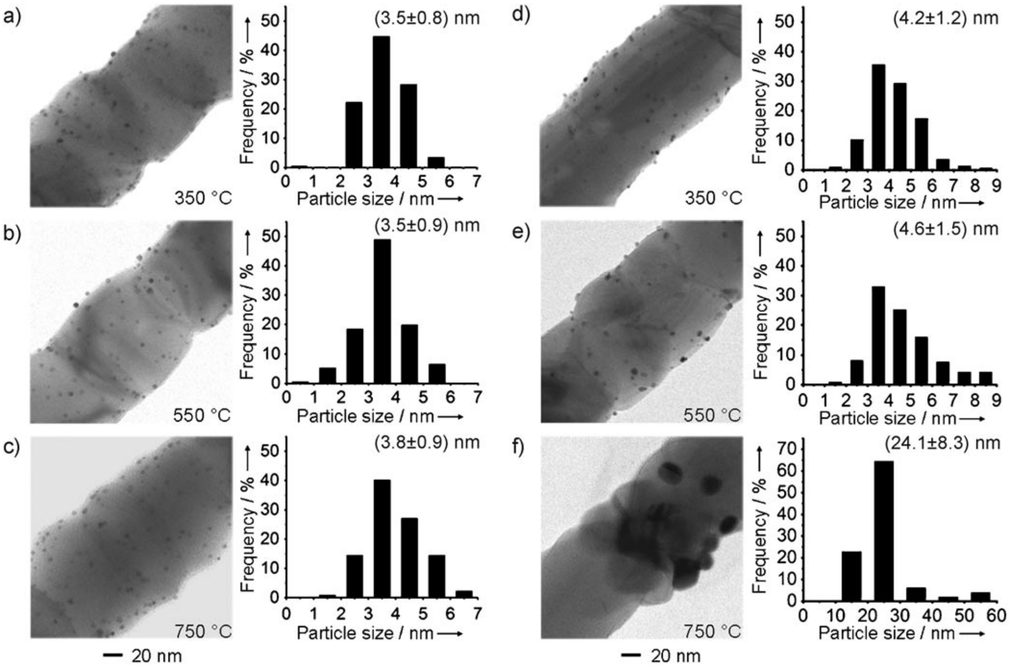

Figure 3. Comparison of thermal stability of the SiO_2/Pt/TiO_2 nanofibers (a–c) and Pt/TiO_2 nanofibers without SiO_2 coating (d–f) at three different calcination temperatures in air for 2 h.

demonstrate that the porous SiO_2 sheath could serve as an effective barrier to prevent the migration of Pt atoms and/or nanoparticles during calcination, thus enabling the Pt nanoparticles to become sinter-resistant. This new catalytic system also exhibited good resistance against sintering in a reducing gas environment such as hydrogen gas (Figure S3 in the Supporting Information).

The effect of Pt loading on the sinter resistance of the porous-SiO_2/Pt/TiO_2 nanofibers was also investigated. In this case, the Pt/TiO_2 nanofibers with a relatively higher Pt loading (ca. 3.6 wt %) were prepared by immersing the calcined TiO_2 nanofibers in the as-prepared suspension of Pt nanoparticles (Figure S4a in the Supporting Information). These nanofibers were coated with porous SiO_2 sheaths using the same procedure as in Figure 2e (Figure S4b in the Supporting Information). This sample exhibited good sinter resistance upon calcination in air up to 550 °C, but sintering started to occur at 750 °C (Figure S5 in the Supporting Information). In this case, sintering could be facilitated by the significant reduction in the nearest-neighbor distance between the Pt nanoparticles.

We also investigated the catalytic property of the Pt nanoparticles embedded in the porous SiO_2 sheaths by employing the hydrogenation of methyl red (an azo dye) as a model reaction (Figure 4a). The hydrogenation of the N=N bond of methyl red breaks the π conjugation of the molecule, thus resulting in a loss of the red color, which can be readily monitored by UV/Vis spectroscopy.[2b,15] Figure 4b shows absorption spectra of a methyl red solution (which was bubbled with H_2 in advance) before and after passing through the porous-SiO_2/Pt/TiO_2 nanofibers. A high conversion was achieved with all the three porous-SiO_2/Pt/TiO_2 nanofiber catalysts prepared by calcination at different temperatures from 350 to 750 °C, thus indicating that both methyl red and hydrogen molecules were able to diffuse through the porous SiO_2 sheaths to the surface of the embedded Pt nanoparticles. The highest catalytic activity was achieved from the porous-SiO_2/Pt/TiO_2 nanofiber catalyst prepared by calcination at 350 °C, with a conversion of 87 %. The conversion dropped slightly to 81 % for the sample calcined at 550 °C and to 61 % for the sample calcined at 750 °C. These reductions in catalytic activity with increasing calcination temperature might also be caused by surface reconstruction of the Pt nanoparticles,[3] as well as densification of the silica coating.[16] We also confirmed the absence of homogeneous catalysis that might arise from partial dissolution of the Pt into the solution by conducting a control experiment in which the methyl red solution was not bubbled with H_2 gas until it was stirred with the catalyst for 2 minutes and then separated from the catalyst by centrifugation. In these experiments, there was essentially no change to the absorption peak (Figure S6 in the Supporting Information). Taken together, these results clearly show that the porous SiO_2 coating was permeable toward chemical species, and that the porous-SiO_2/Pt/TiO_2 nanofibers retained their catalytic properties.

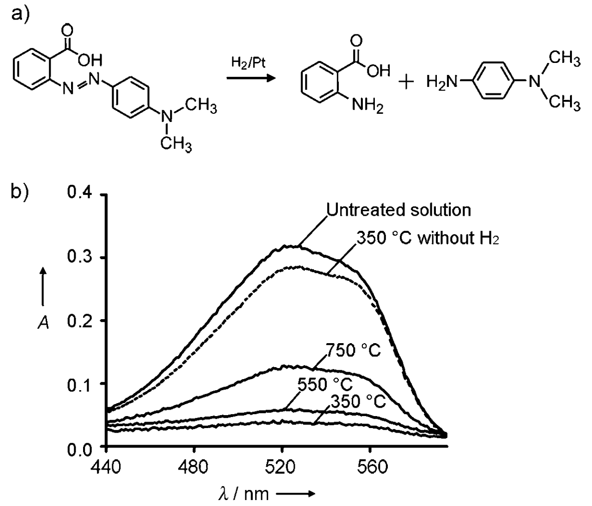

Figure 4. a) Hydrogenation of methyl red. b) UV/Vis spectra of a methyl red solution before and after the hydrogenation reaction with porous-SiO_2/Pt/TiO_2 nanofibers. The conversions were 87 %, 81 %, and 61 % for the porous-SiO_2/Pt/TiO_2 nanofibers obtained by calcination in air for 2 h at 350, 550, and 750 °C, respectively.

In summary, we have demonstrated a sinter-resistant catalytic system based on TiO_2-supported Pt nanoparticles coated by a porous sheath of SiO_2. The porous-SiO_2/Pt/TiO_2 system could resist sintering up to a temperature of 750 °C in air, thus demonstrating the excellent sinter resistance of the catalyst. The porous SiO_2 sheath provides a physical barrier to slow down surface migration for the Pt atoms and/or nanoparticles and thus effectively prevent sintering. Significantly, the porous-SiO_2/Pt/TiO_2 nanofibers were still catalytically active towards hydrogenation of methyl red even after high-temperature calcination, thus demonstrating accessibility of the Pt nanoparticle's surface because of the porous nature of the SiO_2 sheath. The synthetic strategy presented herein should be extendible to other catalytic systems with different compositions.

Received: March 29, 2010
Revised: August 24, 2010
Published online: September 24, 2010

Keywords: nanostructures · platinum · silica · sinter resistance · supported catalysts

---

[1] a) J. Chen, B. Lim, E. P. Lee, Y. Xia, *Nano Today* **2009**, *4*, 81; b) B. Lim, M. Jiang, P. H. C. Camargo, E. C. Cho, J. Tao, X. Lu, Y. Zhu, Y. Xia, *Science* **2009**, *324*, 1302; c) B. Lim, M. Jiang, J. Tao, P. H. C. Camargo, Y. Zhu, Y. Xia, *Adv. Funct. Mater.* **2009**, *19*, 189; d) B. Lim, X. Lu, M. Jiang, P. H. C. Camargo, E. C. Cho, E. P. Lee, Y. Xia, *Nano Lett.* **2008**, *8*, 4043; e) Y. Xia, Y. Xiong, B. Lim, S. E. Skrabalak, *Angew. Chem.* **2009**, *121*, 62; *Angew. Chem. Int. Ed.* **2009**, *48*, 60.

[2] a) E. Formo, P. H. C. Camargo, B. Lim, M. Jiang, Y. Xia, *Chem. Phys. Lett.* **2009**, *476*, 56; b) E. Formo, E. Lee, D. Campbell, Y. Xia, *Nano Lett.* **2008**, *8*, 668; c) E. Formo, Z. M. Peng, E. Lee, X. M. Lu, H. Yang, Y. Xia, *J. Phys. Chem. C* **2008**, *112*, 9970; d) E. Formo, M. S. Yavuz, E. P. Lee, L. Lane, Y. Xia, *J. Mater. Chem.* **2009**, *19*, 3878; e) L. Yang, W. Yang, Q. Cai, *J. Phys. Chem. C* **2007**, *111*, 16613; f) L. Jiang, G. Sun, Z. Zhou, S. Sun, Q. Wang, S. Yan, H. Li, J. Tian, J. Guo, B. Zhou, Q. Xin, *J. Phys.*

Chem. B **2005**, *109*, 8774; g) H. Song, R. M. Rioux, J. D. Hoefelmeyer, R. Komor, K. Niesz, M. Grass, P. Yang, G. A. Somorjai, *J. Am. Chem. Soc.* **2006**, *128*, 3027; h) W. Huang, J. N. Kuhn, C. K. Tsung, Y. Zhang, S. E. Habas, P. Yang, G. A. Somorjai, *Nano Lett.* **2008**, *8*, 2027.

[3] S. H. Joo, J. Y. Park, C. K. Tsung, Y. Yamada, P. Yang, G. A. Somorjai, *Nat. Mater.* **2009**, *8*, 126.

[4] S. Kim, Y. Yin, A. P. Alivisatos, G. A. Somorjai, J. T. Yates, *J. Am. Chem. Soc.* **2007**, *129*, 9510.

[5] H. P. Zhou, H. S. Wu, J. Shen, A. X. Yin, L. D. Sun, C. H. Yan, *J. Am. Chem. Soc.* **2010**, *132*, 4998.

[6] K. T. Li, M. H. Hsu, I. Wang, *Catal. Commun.* **2008**, *9*, 2257.

[7] Q. Zhang, T. Zhang, J. Ge, Y. Yin, *Nano Lett.* **2008**, *8*, 2867.

[8] K. Yu, Z. Wu, Q. Zhao, B. Li, Y. Xie, *J. Phys. Chem. C* **2008**, *112*, 2244.

[9] P. M. Arnal, M. Comotti, F. Schüth, *Angew. Chem.* **2006**, *118*, 8404; *Angew. Chem. Int. Ed.* **2006**, *45*, 8224.

[10] D. Li, Y. Xia, *Nano Lett.* **2003**, *3*, 555.

[11] J. Chen, T. Herricks, M. Geissler, Y. Xia, *J. Am. Chem. Soc.* **2004**, *126*, 10854.

[12] a) Y. Lu, Y. Yin, Z. Y. Li, Y. Xia, *Nano Lett.* **2002**, *2*, 785; b) Y. Yin, Y. Lu, Y. Sun, Y. Xia, *Nano Lett.* **2002**, *2*, 427; c) W. Stöber, A. Fink, E. Bohn, *J. Colloid Interface Sci.* **1968**, *26*, 62.

[13] Y. Borodko, L. Jones, H. Lee, H. Frei, G. Somorjai, *Langmuir* **2009**, *25*, 6665.

[14] M. H. Kim, J. R. Ebner, R. M. Friedman, M. A. Vannice, *J. Catal.* **2001**, *204*, 348.

[15] C. M. Cobley, D. J. Campbell, Y. Xia, *Adv. Mater.* **2008**, *20*, 748.

[16] a) J. Gallardo, P. Galliano, A. Durán, *J. Sol-Gel Sci. Technol.* **2000**, *19*, 393; b) H. Saito, M. Higuchi, K. Katayama, Y. Azuma, *J. Mater. Sci. Lett.* **2003**, *22*, 1419.